CHEMISTRY OF MATERIALS

COMMUNICATION

pubs.acs.org/cm

Bioinspired Magnetite Mineralization of Peptide−Amphiphile Nanofibers

Eli D. Sone[†] and Samuel I. Stupp*

Department of Chemistry, Department of Materials Science & Engineering, Department of Medicine, Institute for BioNanotechnology in Medicine, Northwestern University, Evanston, Illinois 60208-3108, United States

Supporting Information

KEYWORDS: biomaterials, biomineralization, self-assembly and self-assembled materials

The biomineral magnetite (Fe_3O_4) is found in a wide range of organisms, from bacteria to higher vertebrates such as birds and fish, most often functioning as a magnetoreceptor.[1−3] In magnetotactic bacteria, for example, the formation of chains of aligned, single domain Fe_3O_4 nanocrystals (known as magnetosomes) along a filamentous structure, creates a permanent magnetic dipole in each bacterium that enables it to find appropriate oxygen levels in the ocean using the geomagnetic field.[4,5] The biomineralization of the magnetosome involves a remarkable level of control over the magnetite crystals, which are rather uniform in size and morphology in each organism, and crystallographically aligned with respect to the filament axis.

A synthetic approach to the control of morphological features and organization of inorganic substances on the nanoscale is to imitate biology by using organic objects as templates for inorganic growth.[6−11] By mimicking natural systems, one may gain insights into biomineralization mechanisms, and synthesize structures with potentially interesting functions. Biomimetic templating strategies have been applied to magnetite using both biological[12−14] and synthetic[15−19] templates. However, none of these systems has been able to replicate the level of control achieved by magnetotactic bacteria.

Our laboratory developed peptide-amphiphile (PA) molecules that self-assemble into cylindrical fibers 6−8 nm in diameter, leading to the formation of aqueous gels at low concentrations (∼1 wt %).[20−22] PA fibers consisting of an aliphatic interior and peptidic exterior displaying the S(P)RGD sequence have been shown to be versatile mineralization templates; they align crystals of hydroxyapatite,[20,23] thus recreating some of the nanoscale features of bone structure, and can nucleate cadmium sulfide nanocrystals as well.[24] We report here on the self-assembly and mineralization of histidine-containing PAs designed to act as templates for the nucleation and growth of magnetite. The system produces one-dimensional arrays of magnetite nanocrystals that decorate PA fibers, mimicking some aspects of the linear arrangement of magnetite along a filament in bacterial magnetosomes.

Fe_3O_4 is a mixed valence inverse spinel compound with a 1:2 ratio of Fe(II):Fe(III). Its aqueous synthesis under ambient conditions generally involves either partial oxidation of an Fe(II) precursor,[15,25] or use of Fe(II) and Fe(III) precursors in the appropriate ratio.[26,27] Both methods require an acidic pH to dissolve the iron salts, and a subsequent increase in pH to induce precipitation of the oxide. With the partial oxidation method in mind, we originally designed the PA molecule shown below (**1**). Molecule **1** contains three histidine amino acids at its C-terminus that are expected to be exposed at the fiber/water interface upon self-assembly. The histidines are separated from the alkyl tail of the molecule by alanine and glycine residues. Histidine is known to chelate Fe^{2+}, particularly through the lone electron pair on the δ-nitrogen. We thus hoped to create a local supersaturation of Fe^{2+} around the fiber, leading to preferential nucleation and growth of iron oxide on the fiber surface. It is noteworthy that the pK_a of histidine (6.0) is low enough that the δ-nitrogen should be largely deprotonated at a pH where Fe(II) is still soluble, allowing metal ion coordination to take place.

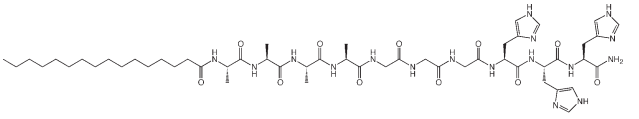

1

Molecule **1** can be solubilized in water at low concentrations (6.7 mg/mL), the resulting solutions having pH ∼2, presumably due to the trifluoroacetate (TFA)-histidine salt that forms upon deprotection of the histidines (see the Supporting Information for experimental details). As expected, **1** self-assembles into fibers as the pH is raised and the histidines are deprotonated, neutralizing the amphiphiles and eliminating electrostatic repulsions. This network of fibers results in the formation of self-supporting gels. Molecule **1** can also be induced to form fibers at acidic pH, by heating the solution to 80 °C, as has been recently observed for other PAs.[28] Upon cooling, the solution forms gels, which were characterized using transmission electron microscopy (TEM). Figure 1a shows 8−10 nm unstained fibers obtained from heat-induced gels of **1**. The high level of contrast for this unstained organic structure is surprising. Increased contrast may arise from TFA counterions that form a salt with the histidines on drying, or from increased order in the heat-induced fibers.[29] In comparison, Figure 1b shows a network of fibers obtained from a pH-induced gel. In this case, the histidines have been deprotonated, and thus no longer form a TFA salt. The level of contrast, wherein bundles of fibers but no individual fibers can be discerned, is similar to what has been observed for other unstained PA fibers. Individual fibers could be resolved from pH-induced samples with negative staining (not shown).

Received: October 16, 2010
Revised: March 16, 2011
Published: March 29, 2011

dx.doi.org/10.1021/cm102985v | *Chem. Mater.* 2011, 23, 2005–2007

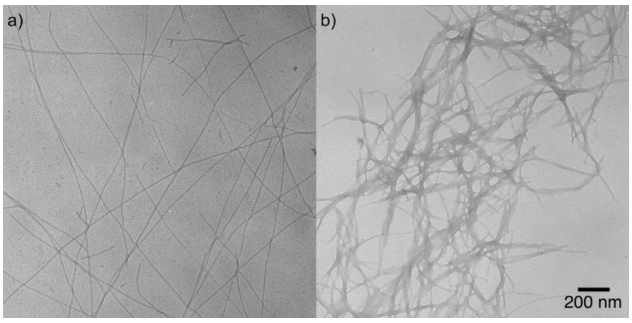

Figure 1. TEM micrographs of unstained nanofibers formed from **1**. (a) Fibers from heat-induced gel. (b) Fibers from pH-induced gel.

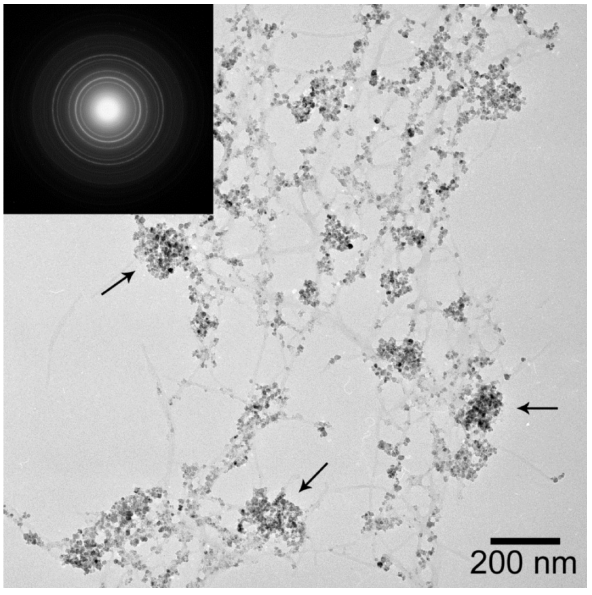

Figure 2. TEM micrograph showing magnetite nanocrystals decorating a network of fibers formed from **1**. Inset shows a selected area diffraction pattern. Arrows indicate clumps of crystals.

Fibers formed by heating of histidine-containing PAs are well suited for mineralization studies, since they form even in acidic media, allowing introduction of iron precursors to suspensions of preformed fibers. The pH can subsequently be raised to induce oxide formation by exposing the suspension to ammonia (NH_3) vapors, without distruption of fiber integrity. We initially attempted mineralizations using $FeCl_2$ as a precursor, but found the partial oxidation process difficult to control precisely, leading to products that were mixtures of iron oxide phases. Subsequent mineralization attempts with a 1:2 ratio of $FeCl_2$:$FeCl_3$ were more successful, yielding a black/brown precipitate that was uniformly responsive to a bar magnet. A representative micrograph of a TEM sample prepared from this mineralization is shown in Figure 2, revealing a network of fibers of **1** selectively decorated with 5−15 nm cuboidal crystals. Electron diffraction (inset) of the sample matches very closely with the expected pattern for magnetite (see the Supporting Information, Table S1). However, it is difficult to make this assignment unambiguously from diffraction data alone, since the pattern for maghemite (γ-Fe_2O_3), a closely related phase, is quite similar. For this reason, we performed Raman spectroscopy in which we observed the characteristic magnetite peak at ~674 cm^{-1} (see the Supporting Information, Figure S1).[30,31] We note that this does not exclude the possibility that some oxidation of magnetite to maghemite has occurred, which is in fact likely because the synthesis is performed in an ambient atmosphere.

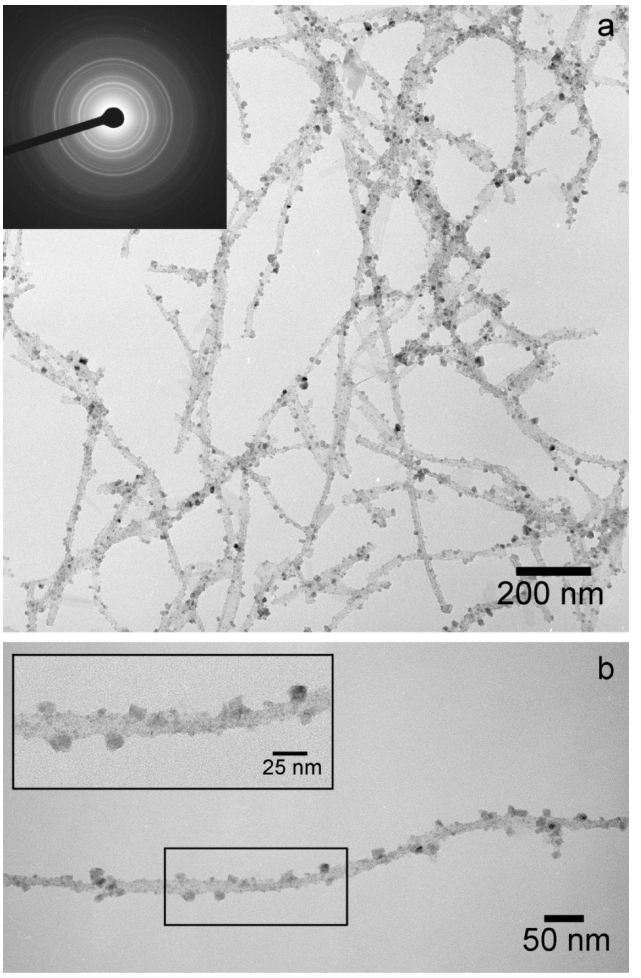

Figure 3. TEM micrograph of magnetite nanocrystals on fibers formed from **2**. (a) Network of magnetite-decorated fibers with inset showing electron diffraction pattern. (b) Crystals grown on an isolated bundle of fibers, with inset showing an enlargement of the boxed portion of the micrograph.

It is evident in Figure 2 that all of the magnetite nanocrystals are associated with the organic network, indicating that the fibers are effective templates. However, a number of the crystals are not attached directly to fibers, but rather form clumps of crystals, as indicated by the arrows. We reasoned that we might improve the templating by including in the PA Fe^{3+} chelation sites, in addition to the Fe^{2+}-binding histidines, because both are used as precursors in the magnetite synthesis. Molecule **2**, shown below, contains an additional aspartic acid residue compared to **1**, and is terminated by a carboxylic acid rather than an amide at the C-terminus. These two carboxylic acid groups are expected to act as coordination sites for Fe^{3+}.

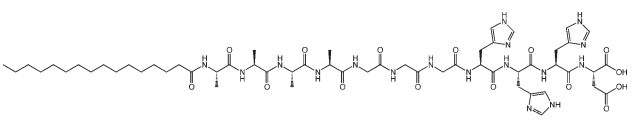

2

Like its amide-terminated counterpart, **2** can also be induced to self-assemble at acidic pH by heating to 80 °C, forming gels at a concentration of 10 mg/mL. Suspensions of fibers from heat-induced gels were mineralized according to the same

procedure used for **1**, and likewise produced a black/brown precipitate that was also uniformly responsive to a bar magnet. Figure 3a shows 10−20 nm cuboidal nanocrystals decorating a network of fibers of molecule **2** obtained from this suspension 1.5 h after exposure to NH_3 vapors. Electron diffraction from this sample (inset) also corresponds well to the pattern expected for magnetite. We note that more of the particles in this sample are in direct contact with the fibers than in the mineralized sample of **1** (Figure 2). Furthermore, the fibers are much more evident because of numerous small particles ∼2 nm in size that cover their surface. We interpret these particles as precursors to the larger, faceted crystals that are evident. It is not clear whether the small particles are amorphous or crystalline. The presence of these small particles on the fibers suggests that nucleation and growth may take place on the fibers themselves, rather than crystals nucleating and growing in solution, and only subsequently attaching to the fibers.[32] Figure 3b shows an isolated strand covered by nanocrystals, emphasizing the resemblance of the linear arrangement of particles along the fibers to chains of magnetite particles in magnetotactic bacteria. The width of the strand (10−20 nm) suggests it is made of more than one fiber in places. The inset shows more clearly the close association of the faceted crystals with the PA fiber, as well as the smaller, nonfaceted particles. We did not, however, observe any preferred crystallographic alignment of the crystals on the fibers, as is found in bacterial magnetosomes. Moreover, magnetite crystals in magnetosomes are typically significantly larger (∼50 nm) than the synthetic crystals (10−20 nm).

We have shown that histidine-rich PA fibers are effective templates for the growth of magnetite nanocrystals. Fibers containing both Fe^{3+} and Fe^{2+} binding sites were found have a larger portion of directly associated crystals than those containing only Fe^{2+} binding sites. The PA-magnetite assemblies mimick the linear arrangement of magnetite crystals along a filamentous structure found in bacterial magnetosomes. However, they do not mimick the crystallographic alignment of the crystals that is central to the function of magnetite in magnetotactic bacteria. Synthetic control of magnetite aligment may eventually be accomplished by design of fibers engineered to match a particular face of the magnetite crystal structure.

■ ASSOCIATED CONTENT

Supporting Information. Electron diffraction data, Raman spectrum, and experimental details (PDF). This material is available free of charge via the Internet at http://pubs.acs.org

■ AUTHOR INFORMATION

Corresponding Author

*E-mail: s-stupp@northwestern.edu.

Present Addresses

†Faculty of Dentistry, Department of Materials Science & Engineering, Institute of Biomaterials & Biomedical Engineering, University of Toronto, Toronto, ON M5S 3G9, Canada.

■ ACKNOWLEDGMENT

This work and was supported by the U.S. Department of Energy (DOE) under Award DE-FG02-00ER45810 and made use of the Electron Probe Instrumentation Center, the Analytical Services Laboratory and the Keck Biophysics Facility at Northwestern University. EDS is grateful to the Natural Sciences and Engineering Research Council of Canada for a postgraduate scholarship. We thank Adam McFarland for providing a Raman spectrum, and Jeffrey Hartgerink for helpful discussions.

■ REFERENCES

(1) Kirschvink, J. L.; Walker, M. M.; Diebel, C. E. *Curr. Opin. Neurobiol.* **2001**, *11*, 462.

(2) Mann, S. *Biomineralization: Principles and Concepts in Bioinorganic Materials Chemistry*; Oxford University Press: Oxford, U.K., 2001.

(3) Lowenstam, H. A.; Weiner, S., *On Biomineralization*. Oxford University Press: Oxford, 1989.

(4) Schuler, D.; Frankel, R. B. *Appl. Micribiol. Biotechnol.* **1999**, *52*, 464.

(5) Scheffel, A.; Gruska, M.; Faivre, D.; Linaroudis, A.; Plitzko, J. M.; Schuler, D. *Nature* **2006**, *440*, 110.

(6) Mann, S.; Ozin, G. A. *Nature* **1996**, *382*, 313.

(7) Braun, P. V.; Osenar, P.; Stupp, S. I. *Nature* **1996**, *380*, 325.

(8) Osenar, P.; Braun, P. V.; Stupp, S. I. *Adv. Mater.* **1996**, *8*, 1022.

(9) Estroff, L. A.; Hamilton, A. D. *Chem. Mater.* **2001**, *13*, 3227.

(10) van Bommel, K. J. C.; Friggeri, A.; Shinkai, S. *Angew. Chem., Int. Ed.* **2003**, *42*, 980.

(11) Palmer, L. C.; Newcomb, C. J.; Kaltz, S. R.; Spoerke, E. D.; Stupp, S. I. *Chem. Rev.* **2008**, *108*, 4754.

(12) Wong, K. K. W.; Douglas, T.; Gider, S.; Awschalom, D. D.; Mann, S. *Chem. Mater.* **1998**, *10*, 279.

(13) Archibald, D. D.; Mann, S. *Nature* **1993**, *364*, 430.

(14) Meldrum, F. C.; Heywood, B. R.; Mann, S. *Science* **1992**, *257*, 522.

(15) Abe, M.; Ishihara, T.; Kitamoto, Y. *J. Appl. Phys.* **1999**, *85*, 5705.

(16) Rabelo, D.; Lima, E. C. D.; Reis, A. C.; Nunes, W. C.; Novak, M. A.; Garg, V. K.; Oliveira, A. C.; Morais, P. C. *Nano Lett.* **2001**, *1*, 105.

(17) Sinha, A.; Chakraborty, J.; Das, S. K.; Das, S.; Rao, V.; Ramachandrarao, P. *Mater. Trans.* **2001**, *42*, 1672.

(18) Zhang, Z. M.; Wan, M. X. *Synth. Met.* **2003**, *132*, 205.

(19) Harris, L. A.; Goff, J. D.; Carmichael, A. Y.; Riffle, J. S.; Harburn, J. J.; St. Pierre, T. G.; Saunders, M. *Chem. Mater.* **2003**, *15*, 1367.

(20) Hartgerink, J. D.; Beniash, E.; Stupp, S. I. *Science* **2001**, *294*, 1684.

(21) Hartgerink, J. D.; Beniash, E.; Stupp, S. I. *Proc. Natl. Acad. Sci. U. S. A.* **2002**, *99*, 5133.

(22) Niece, K. L.; Hartgerink, J. D.; Donners, J.; Stupp, S. I. *J. Am. Chem. Soc.* **2003**, *125*, 7146.

(23) Spoerke, E. D.; Anthony, S. G.; Stupp, S. I. *Adv. Mater.* **2009**, *21*, 425.

(24) Sone, E. D.; Stupp, S. I. *J. Am. Chem. Soc.* **2004**, *126*, 12756.

(25) Nishimura, K.; Kohara, Y.; Kitamoto, Y.; Abe, M. *J. Appl. Phys.* **2000**, *87*, 7127.

(26) Massart, R. *IEEE Trans. Magn.* **1981**, *17*, 1247.

(27) Berger, P.; Adelman, N. B.; Beckman, K. J.; Campbell, D. J.; Ellis, A. B.; Lisensky, G. C. *J. Chem. Educ.* **1999**, *76*, 943.

(28) Zhang, S.; Greenfield, M. A.; Mata, A.; Palmer, L. C.; Bitton, R.; Mantei, J. R.; Aparicio, C.; Olvera de la Cruz, M.; Stupp, S. I. *Nat. Mater.* **2010**, *9*, 594.

(29) In some micrographs of unstained fibers, we observed less electron density in the middle of the fiber. This is consistent with presence of TFA on the periphery of the fibe in proximity to histidines, or could reflect increased order in the exterior of the fibers, which is also suggested by their straightness.

(30) de Faria, D. L. A.; Silva, S. V.; de Oliveira, M. T. *J. Raman Spectrosc.* **1997**, *28*, 873.

(31) Tang, J.; Myers, M.; Bosnick, K. A.; Brus, L. E. *J. Phys. Chem. B* **2003**, *107*, 7501.

(32) Similar precrystals were observed on samples of mineralized PA 1 at a similar time interval, although to a lesser extent.